



# Computer analysis of the cemented carbides' microstructure

D. G. Kagramanyan<sup>1</sup>, E. P. Konstantinova<sup>1</sup>, A. N. Nekrasov<sup>2</sup>,

B. B. Straumal<sup>†,3,4,5</sup>, I. Yu. Konyashin<sup>5</sup>, L. N. Shchur<sup>1,6</sup>

<sup>†</sup>straumal@issp.ac.ru

<sup>1</sup>“Higher School of Economics” University, Moscow, 101000, Russia

<sup>2</sup>Korzhinsky Institute of Experimental Mineralogy, RAS, Chernogolovka, 142432, Russia

<sup>3</sup>Science Center in Chernogolovka (SCC), RAS, Chernogolovka, 142432, Russia

<sup>4</sup>Osipyan Institute of Solid State Physics (ISSP), RAS, Chernogolovka, 142432, Russia

<sup>5</sup>National University of Science and Technology MISiS, Moscow, 119049, Russia

<sup>6</sup>Landau Institute for Theoretical Physics (LITP), RAS, Chernogolovka, 142432, Russia

Cemented carbides have been known for about a hundred years and are now widely used in mining, civil and road construction, and mechanical engineering. Their improvement requires the development of novel technologies based on fundamentally new approaches. Here the method for microstructure analysis using computer processing with elements of machine learning and artificial intelligence is proposed. It has been applied to the analysis of micrographs obtained by the scanning electron microscopy of the WC-Co cemented carbides. The geometric parameters of the WC/Co interphase boundaries are extracted using mathematical methods for processing digital pictures. This method is applied to the micrographs of three samples with different WC mean grain sizes. It has been found that the distribution of the contact angles of WC/Co interphase boundaries has a pronounced bimodal structure, and the values of the peak angles are practically the same for the samples of the fine-, medium-, and coarse-grain cemented carbide grades. The distributions of the semiaxes for the isolated areas of the cobalt binder are also obtained. The probability of finding a particular value of long and short semiaxis decreases exponentially with increasing semiaxis length. Contrary to the contact angles, the exponents are different for samples with different WC grain sizes. The obtained results are discussed using the ideas of wetting of grain boundaries and faceting-roughening of interphase boundaries.

**Keywords:** cemented carbides, cobalt binder, interphase boundaries, machine learning, wetting, faceting-roughening.

УДК: 539.5

## Компьютерный анализ микроструктуры твёрдых сплавов на основе карбида вольфрама

Каграманян Д. Г.<sup>1</sup>, Константинова Е. П.<sup>1</sup>, Некрасов А. Н.<sup>2</sup>,

Страумал Б. Б.<sup>†,3,4,5</sup>, Коняшин И. Ю.<sup>5</sup>, Щур Л. Н.<sup>1,6</sup>

<sup>1</sup>Университет «Высшая школа экономики», Москва, 101000, Россия

<sup>2</sup>Институт экспериментальной минералогии им. Коржинского РАН, Черногоровка, 142432, Россия

<sup>3</sup>Научный центр РАН в Черногоровке, Черногоровка, 142432, Россия

<sup>4</sup>Институт физики твёрдого тела им. Осипяна РАН, Черногоровка, 142432, Россия

<sup>5</sup>Национальный исследовательский технологический университет «МИСиС», Москва, 119049, Россия

<sup>6</sup>Институт теоретической физики им. Ландау РАН, Черногоровка, 142432, Россия

Твёрдые сплавы на основе карбида вольфрама известны около ста лет и в настоящее время широко используются в горнодобывающей промышленности, гражданском и дорожном строительстве, а также в машиностроении. Их совершенствование требует разработки новых технологий, основанных на принципиально новых подходах. Предлагается метод анализа микроструктуры с использованием компьютерной обработки с элементами машинного обучения и искусственного интеллекта. Он был применен для анализа микроснимков твёрдых сплавов на основе карбида вольфрама WC-Co, полученных с помощью сканирующей электронной микроскопии. Геометрические

параметры межфазных границ WC/Co извлекаются с помощью математических методов обработки цифровых изображений. Этот метод применен к микроснимкам трех образцов с различным средним размером зерна WC. Установлено, что распределение краевых углов межфазных границ WC/Co имеет ярко выраженную бимодальную структуру, а значения углов пиков практически одинаковы для образцов мелко-, средне- и крупнозернистых твёрдых сплавов на основе карбида вольфрама. Получены также распределения полуосей для изолированных участков кобальтовой связки. Вероятность нахождения конкретного значения длинной и короткой полуосей экспоненциально уменьшается с увеличением длины полуоси. В отличие от углов смачивания, показатели степени различны для образцов с разным размером зерен WC. Полученные результаты обсуждаются с использованием идей смачивания границ зерен и фасетирования/потери огранки межфазных границ.

**Ключевые слова:** цементированные карбиды, кобальтовая связка, межфазные границы, машинное обучение, смачивание, фасетирование/потери огранки.

## 1. Introduction

Materials based on tungsten carbide with a cobalt binder (cemented carbides) have been known for about a hundred years. Cemented carbides are now widely used in mining, civil and road construction, mechanical engineering, etc. [1, 2]. They allow drilling wells of the several kilometres in depth, on the one hand, and bores of several hundred microns in diameter on the other hand. Improving the properties of cemented carbides requires the development of novel technologies based on fundamentally new approaches [3–6]. This article is devoted to one of these new approaches to the analysis of structures with elements of artificial intelligence.

Tungsten carbide itself has a very high hardness, however, it is quite brittle [7,8]. Therefore, cemented carbide is a material composed of tungsten carbide grains imbedded in a cobalt-based binder [9–11]. To obtain the required level of properties (e.g. hardness, wear resistance, fracture toughness, etc.) needed for various applications, it is necessary to vary the proportion of cobalt binder in the material, as well as the grain size of tungsten carbide [12–16]. For the further development of this class of materials, the usual parameters for describing its microstructure, which are used in quantitative metallography, such as the average grain size or the volume fraction of phases, are insufficient [17–19]. For example, they are not able to take into account the peculiarities of grain and interphase boundaries [20, 21]. It is necessary to develop more subtle methods to characterize the features of the topology of the mutual penetration of the WC and Co phases [22–24]. This paper is dedicated to the first steps on this direction.

The use of machine learning to analyse the geometric properties of the parameters of the topology of the mutual penetration of the WC and Co phases turned out to be a non-trivial task requiring the use of a set of image processing methods. Bulgarevich et al. estimated the percentage of iron and impurities in steel using the machine learning [25]. It has been done by counting the number of pixels, which is a standard image processing technique. The properties of cemented carbide are determined by a set of microstructure parameters. The contact angle spectra at triple junctions of WC/WC grain boundaries and WC/Co interphase boundaries provide information on complete and incomplete wetting by the melt or on the presence of a second carbide phase. Revealing the connectivity of chains of grains of the same phase in two- and multiphase materials may indicate the

presence or absence of the percolation phenomenon. In other words, for the analysis of cemented carbide, it is necessary to analyse the geometric properties of WC and Co grains and the boundaries between them. In [26] a method has been proposed for determining contact angles in triple joints of grains by the line segments passing along the grain boundary, however, for its application, it is necessary to first determine this boundary, which is not discussed in [26]. We were unable to find a method for determining grain boundaries in the available scientific literature.

In this paper, we propose the use of a set of methods and algorithms, the sequential application of which makes it possible to solve the problem of determining the contact angles of WC/WC grain boundaries and the geometry of cobalt binder areas. It turned out that the problem of determining the boundaries of the cobalt binder can be carried out more reliably than the problem of determining the WC/WC grain boundaries. This is due to the fact that a noticeable part of the WC grains has a tight contiguity, which cannot be unambiguously distinguished when processing the images at our disposal. We demonstrate our method applied to three images of fine-, medium- and coarse-grained cemented carbide specimens.

## 2. Experimental

According to the method described earlier, samples of cemented carbide with fine, medium and coarse WC grains were prepared [27–29]. The samples were made from a mixture of tungsten carbide powder with different grain sizes and cobalt powder with an average grain size of about one micron. The powders were milled in ball mills with WC-Co balls in hexane at a ball-to-powder ratio of 6:1 with 2 wt.% of paraffin wax for 20 hours. After drying, the suspension obtained in such a way was sieved to obtain WC-Co powders, and such powders were used to compress green specimens (cylinders) with a diameter of about 20 mm and a height of 5 mm. The pressed samples were sintered in a vacuum furnace at a temperature of 1400°C for one hour. Samples for structural studies were mechanically ground and polished with diamond paste with a grain size of 1 µm. The obtained cross-sections underwent microscopic examination using scanning electron microscopy (SEM) and X-ray microanalysis on a Tescan Vega TS5130 MM device equipped with an energy dispersive LINK spectrometer manufactured by Oxford Instruments. The digital image size was 3072 by 1680 pixels, and each pixel has 256 shades of gray.

### 3. Results and discussion

#### 3.1. Image preprocessing

We used digital micrographs obtained by SEM in reflected electrons mode (Fig. 1a). The image was smoothed with a weighted median filter [30] to suppress random noise and point artifacts. To increase the contrast of WC/WC grain boundaries and cobalt binder, the Otsu binarization algorithm [31] was used, which converts an image with 256 shades of color into a one-bit image with two colors. Then the binarized image was passed through the Sobel filter [32]. It returns a gradient map of the image that highlights well the pixel contrast transition. The last stage is the addition of the binarized image and the gradient map. It is necessary to explicitly highlight the pixels in the WC/Co boundary zone. After preprocessing, the image pixels have three values: 0 is for WC, 1 is for cobalt binder, and 2 is for boundary region between WC and Co.

#### 3.2. Contour detection

The boundaries of the binder phase were selected in the image by applying the Kenny operator [33] to the preprocessed image. For convenience, let us number the pixels of the border contour clockwise using the convolution matrix [34]. For further analysis, one needs not the entire set of points, but only corner points and breakpoints, which characterize entirely the piecewise smooth boundary. For this, we use the Ramer-Douglas-Pecker algorithm [35]. An example of the resulting analysis is shown in Fig. 1b.

#### 3.3. Angles distribution

The calculation of the angles between the sides of the cobalt binder region is based on the dot product. Choose three points of the contour  $x^1, x^2, x^3$  coming one after another and

compose two vectors  $\mathbf{a} = (x_1^2 - x_1^1, x_2^2 - x_2^1, 0)$  and  $\mathbf{b} = (x_1^3 - x_1^2, x_2^3 - x_2^2, 0)$ . The angle  $\phi$  between  $\mathbf{a}$  and  $\mathbf{b}$  is calculated by the formula  $\phi = \arccos((\mathbf{a}, \mathbf{b}) / (|\mathbf{a}| |\mathbf{b}|))$ . To determine whether an angle  $\phi$  belongs to a sector less than  $\pi$  or more than  $\pi$ , we use a triple of vectors  $\mathbf{a}, \mathbf{b}, \mathbf{c}$ , where  $\mathbf{c} = [\mathbf{a}, \mathbf{b}]$ . We use the sign of the determinant  $D$ , composed of the coordinates of the vectors  $\mathbf{a}$  and  $\mathbf{b}$ ,  $D = [\mathbf{a}, \mathbf{b}]$ . Iteratively passing along all the contours, we obtain the values of the angles formed by the WC/Co boundaries contours.

For each of the three studied samples, we plotted a histogram of angles. The normalized angles distribution density is shown in Fig. 2. Solid curves are the bimodal approximation of these data. Interestingly, the positions of peaks are approximately the same for all three samples, within

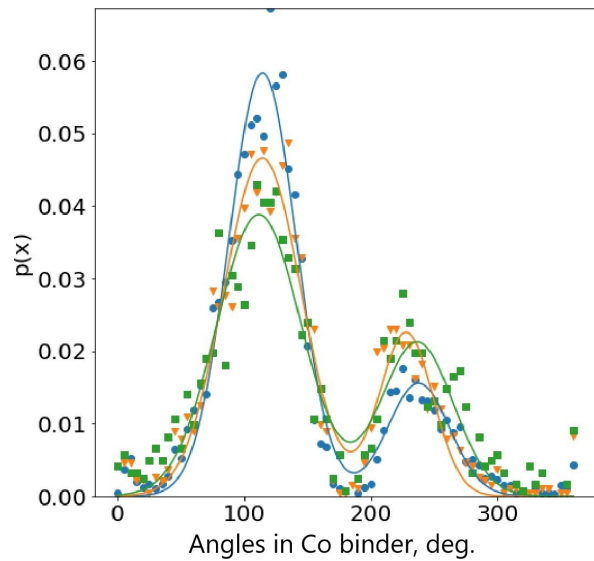
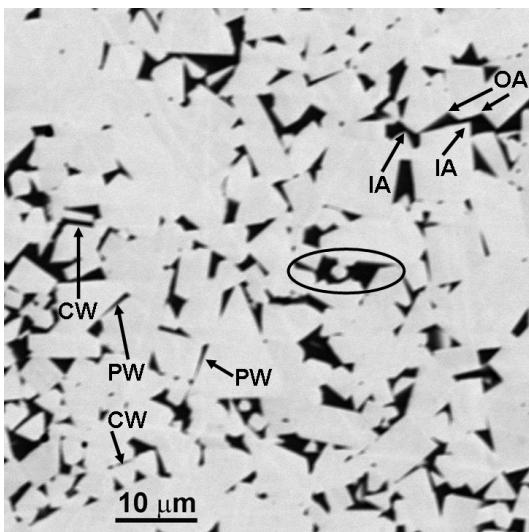
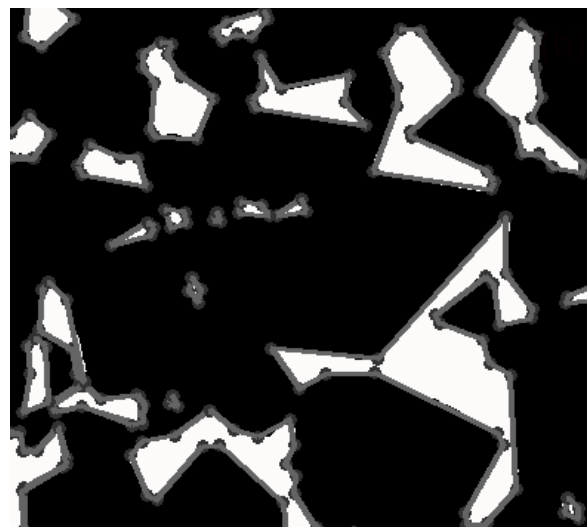


**Fig. 2.** (Color online) Distribution of angles along WC/Co interphase boundaries for the three samples with different WC grain sizes: large (green squares), medium (orange triangles), and small (blue circles) grains. Solid colored lines give the bimodal approximation to the corresponding experimental data.



a



b

**Fig. 1.** SEM micrograph of WC-Co cemented carbide with coarse WC grains. Ellipse marks the example of the analyzed “island” Co grains. CW and PW mark the example of WC/WC GBs completely and partially wetted by a Co binder. IA and OA are incoming and outgoing angles in the cobalt binder (a). An example of a fragment of a preprocessed image. Light areas correspond to cobalt binder, and the dark areas correspond to WC grains. Gray is the linearly approximated contours of the WC/Co boundaries (b).

the limits of the available accuracy. High peaks correspond to angles of  $\approx 114^\circ$ , and low peaks to angles of  $\approx 235^\circ$ . The angles below  $180^\circ$  correspond to those places where the cobalt binder forms triple joints with WC/WC grain boundaries (so-called “outcoming” angles, OA in Fig. 1). In [36,37], such contact angles were measured “manually” using SEM micrographs. The spectrum of these angles is controlled by the phenomena related with grain boundary wetting as well as with differences between special and general grain boundaries [38–41]. Angles ranging from  $180^\circ$  to  $360^\circ$  can be called “incoming” (IA in Fig. 1). These are the places where the edges of WC crystals seem to penetrate the cobalt binder. These angles are determined not by WC/WC GBs but by the natural faceting of differently rotated WC crystallites [42]. It is interesting to note that the sum of the values of the two maxima ( $114^\circ$  and  $235^\circ$ ) is close to  $360^\circ$ . However, the physical nature of peaks is different. As we noted above, these peaks correspond to the “outgoing” and “incoming” angles between the carbide grains and the metal binder; most likely, they are determined mainly by the equilibrium shape of the faceted tungsten carbide crystals and the angles on the corresponding edges between the flat faces.

### 3.4. Determining the semiaxes of polygons

To determine the width and length of the cobalt binder region, we plot an ellipse around the points of the contour (Fig. 1). To do this, we applied the algorithm for finding a point lying at the intersection of convex sets [43], which constructs a set of ellipsoids and chooses the smallest of them, but at the same time covering the largest possible number of contour points. By iteratively going over all the previously selected contours, we obtain the distributions of the semiaxes of the sought ellipses (see Fig. 3). The probability  $r$  of longer semiaxes is distributed according to the exponential law  $P(r) \propto \exp -r/r_0$  with an approximate value of  $r_0 = 1, 2$ , and  $3 \mu\text{m}$  for alloys with small, medium, and large grain sizes, respectively. It has to be underlined that the exponents are different for the samples with different WC mean grain sizes.

Interestingly, our technique, applied to only three typical samples, has already allowed us to obtain a new result in the field of materials science, namely the presence of a

bimodal distribution. Moreover, the values of the angles corresponding to the distribution peaks are the same for samples with different grain sizes of tungsten carbide, which is an essential feature of the WC/Co material. This feature, which needs to be confirmed when examining a material with more significant variability, may turn out to be a kind of material identifier.

The analysis of a much larger number of images will also allow us to search for correlations between the values of geometric quantities calculated by us and the strength and mechanical characteristics measured by experimental methods. We plan to carry out such an analysis by developing computer processing techniques using deep neural network technology.

## 4. Conclusions and outlook

A set of methods has been proposed to process the microstructure images of cemented carbide consisting of tungsten carbide grains in a cobalt binder. The shape of interphase boundaries between WC grains and Co binder has been analyzed. The “incoming” and “outcoming” contact angles in the breakpoints of these interphase boundaries have been determined. The distribution of these contact angles is bimodal, with maxima at  $114^\circ$  and  $235^\circ$ . The position of both maxima does not depend on the WC grain size. The semiaxes of “islands” of cobalt binder have also been measured. The probability of finding a particular value of long and short semiaxis decreases exponentially with increasing semiaxis length. Contrary to the contact angles, the exponents are different for samples with different WC grains sizes.

Based on the obtained results, we plan to conduct training of neural networks and subsequent testing on various cemented carbide samples. For the study, we plan to use a set of available neural networks (f.e., fully connected and generative) to conduct multi-criteria analysis. The goal is to identify correlations between the geometric properties, the determination method described in this article, and the mechanical and physical parameters of the material.

*Acknowledgments.* Computations were done using the CHARISMa supercomputer at the HSE University. The analysis

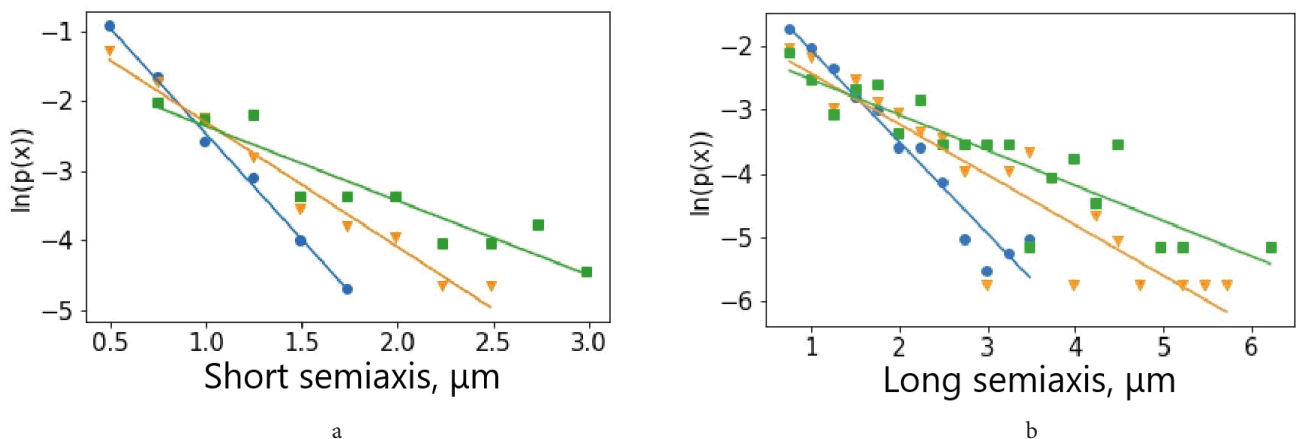


**Fig. 3.** (Color online) Distribution of semiaxes of cobalt binder for three samples with different WC mean grain size (same colors and symbols as in Fig. 2). The vertical axis shows the logarithms of the distribution probability. Straight lines are the exponential approximation of the corresponding experimental data.

was carried out within the framework of the state assignment of the Ministry of Education and Science of the Russian Federation at the LITP (LS) within the Project Teams framework of MIEM HSE (DK and EK). One of the co-authors (IK) gratefully acknowledges the financial support from the Russian Foundation for Basic Research (Project No. 20-08-00750). BS gratefully acknowledges the financial support from the Ministry of Education and Science of the Russian Federation contract no. 075-15-2021-999.

## References

- H. Zhang, J. Xiong, Z. Guo, T. Yang, J. Liu, T. Hua. *Ceramics International*. 47, 26050 (2021). [Crossref](#)
- C. Edtmaier, M. Wolf, R. de Oro Calderon, W.-D. Schubert. *Int. J. Refract. Met. Hard Mater.* 100, 105652 (2021). [Crossref](#)
- M. Mariani, I. Goncharov, D. Mariani, G. P. De Gaudenzi, A. Popovich, N. Lecis, M. Vedani. *Int. J. Refract. Met. Hard Mater.* 100, 105639 (2021). [Crossref](#)
- J.-H. Lee, S.-K. Hong, H.-K. Park. *Int. J. Refract. Met. Hard Mater.* 100, 105649 (2021). [Crossref](#)
- K.-W. Kim, G.-S. Ham, S.-H. Park, J.-W. Cho, K.-A. Lee. *Int. J. Refract. Met. Hard Mater.* 99, 105591 (2021). [Crossref](#)
- K.-F. Wang, X.-H. Yang, K.-C. Chou, G.-H. Zhang. *Int. J. Refract. Met. Hard Mater.* 98, 105569 (2021). [Crossref](#)
- H. Fei, H. Wu, X. Yang, B. Xing, Y. Yang, J. Xiong, J. Liu. *Int. J. Refract. Met. Hard Mater.* 98, 105545 (2021). [Crossref](#)
- Y. Yang, Y. Yang, C. Liao, G. Yang, Y. Qin, Q. Q. Li, M. Wu. *Tribology International*. 161, 107086 (2021). [Crossref](#)
- K. Wang, K. Zhao, J. Liu, D. Liu, T. Li, W. Li, Z. Sun, L. An. *Ceramics International*. 47, 20731 (2021). [Crossref](#)
- K.E. Agode, C. Wolff, M. Nouari, A. Moufki. *Int. J. Refract. Met. Hard Mater.* 99, 105588 (2021). [Crossref](#)
- K. Maier, T. Klünsner, M. Krobath, P. Pichler, S. Marsoner, W. Ecker, C. Czettel, J. Schäfer, R. Ebner. *Int. J. Refract. Met. Hard Mater.* 100, 105633 (2021). [Crossref](#)
- Z. Z. Fang, X. Wang, T. Ryu, K. S. Hwang, H. Y. Sohn. *Int. J. Refr. Met. Hard Mater.* 27, 288 (2009). [Crossref](#)
- H. Li, Y. Du, J. Long, Z. Ye, Z. Zheng, H. Zapolsky, G. Demange, Z. Jin, Y. Peng. *Computational Materials Science*. 196, 110526 (2021). [Crossref](#)
- C. Qian, K. Li, H. Cheng, W. Zhang, X. Jiang, Y. Liu. *Int. J. Refract. Met. Hard Mater.* 98, 105547 (2021). [Crossref](#)
- J. Chen, L. Zhou, J. Liang, B. Liu, J. Liu, R. Chen, X. Deng, S. Wu, M. Huang. *Materials Chemistry and Physics*. 271, 124919 (2021). [Crossref](#)
- P. Pereira, L. M. Vilhena, J. Sacramento, A. M. R. Senos, L. F. Malheiros, A. Ramalho. *Wear*. 482–483, 203924 (2021). [Crossref](#)
- Q. Zhang, K. Huang, J. Wang, L. Wang, M. Yuan, Y. Tian, L. Ouyang. *Ceramics International*. 47, 22683 (2021). [Crossref](#)
- B. Han, W. Dong, B. Fan, S. Zhu. *RSC Adv.* 11, 22495 (2021). [Crossref](#)
- Y. Yang, L. M. Luo, X. Zan, X. Y. Zhu, L. Zhu, Y. C. Wu. *Int. J. Refract. Met. Hard Mater.* 98, 105536 (2021). [Crossref](#)
- S. Lay. *Int. J. Refract. Met. Hard Mater.* 99, 105584 (2021). [Crossref](#)
- K. Lu, C. Shen, Y. He, S. Huang, Y. Ba. *Int. J. Refract. Met. Hard Mater.* 98, 105563 (2021). [Crossref](#)
- E. Fransson, M. Gren, G. Wahnström. *Acta Materialia*. 216, 117128 (2021). [Crossref](#)
- T. Yang, K. Shi, X. Liu, J. Sang, X. Xia, W. Su, J. Ren, R. Zhang, B. Xing. *Int. J. Refract. Met. Hard Mater.* 98, 105548 (2021). [Crossref](#)
- K. Wang, R. Wang, X. Zhou, G. Li, J. Pei, Q. Wang. *Int. J. Refract. Met. Hard Mater.* 100, 105630 (2021). [Crossref](#)
- D. S. Bulgarevich, S. Tsukamoto, T. Kasuya, M. Demura, M. Watanabe. *Sci. Rep.* 8, 2078 (2018). [Crossref](#)
- M. Chandross, E. A. Holm. *Metal. Mater. Trans. A*. 41, 3018 (2010). [Crossref](#)
- I. Konyashin, B. Ries, S. Hlawatschek, A. Mazilkin. *Int. J. Refr. Met. Hard Mater.* 71, 357 (2018). [Crossref](#)
- I. Konyashin, B. Ries, F. Lachmann, R. Cooper, A. Mazilkin, B. Straumal, A. Aretz, V. Babaev. *Int. J. Refr. Met. Hard Mater.* 26, 583 (2008). [Crossref](#)
- I. Konyashin, B. Ries, F. Lachmann, A. T. Fry. *J. Mater. Sci.* 47, 7072 (2012). [Crossref](#)
- D. R. K. Brownrigg. *Comm. ACM.* 27, 807 (1984). [Crossref](#)
- O. Nobuyuki. *IEEE Trans. Systems, Man & Cyber.* 9, 62 (1979). [Crossref](#)
- H. Farid, E. P. Simoncelli. Optimally rotation-equivariant directional derivative kernels. In: *Computer Analysis of Images and Patterns* (ed. by G. Sommer, K. Daniilidis, J. Pauli). *Lecture Notes in Computer Science*. Springer, Berlin, Heidelberg (1997) 296 p. [Crossref](#)
- W. Rong, Z. Li, W. Zhang, L. Sun. 2014 IEEE International Conference on Mechatronics and Automation. Tianjin, China (2014) p. 577. [Crossref](#)
- S. Suzuki, K. Abe. *Comp. Vis. Graph. Image Proc.* 30, 32 (1985). [Crossref](#)
- H. John, S. Jack. *Speeding Up the Douglas-Peucker Line-Simplification Algorithm*. Vancouver, CiteSeerX (1992).
- I. Konyashin, B. Ries, D. Hlawatschek, Y. Zhuk, A. Mazilkin, B. Straumal, F. Dorn, D. Park. *Int. J. Refract. Met. Hard Mater.* 49, 203 (2015). [Crossref](#)
- I. Konyashin, B. B. Straumal, B. Ries, M. F. Bulatov, K. I. Kolesnikova. *Mater. Lett.* 196, 1 (2017). [Crossref](#)
- E. I. Rabkin, L. S. Shvindlerman, B. B. Straumal. *Int. J. Mod. Phys. B*. 5, 2989 (1991). [Crossref](#)
- E. L. Maksimova, L. S. Shvindlerman, B. B. Straumal. *Acta metall.* 36, 1573 (1988). [Crossref](#)
- F. Ernst, M. W. Finnis, A. Koch, C. Schmidt, B. Straumal, W. Gust. *Z. Metallk.* 87, 911 (1996).
- J. Schölhammer, B. Baretzky, W. Gust, E. Mittemeijer, B. Straumal. *Interf. Sci.* 9, 43 (2001). [Crossref](#)
- B. B. Straumal, O. A. Kogtenkova, A. S. Gornakova, V. Sursaeva, B. Baretzky. *J. Mater. Sci.* 51, 382 (2016). [Crossref](#)
- M. Grötschel, L. Lovász, A. Schrijver. *The Ellipsoid Method*. In: *Geometric Algorithms and Combinatorial Optimization*. Algorithms and Combinatorics. Heidelberg, Springer (1993). [Crossref](#)